

Flexible Biosensors for the Impedimetric Detection of Protein Targets Using Silk-Conductive Polymer Biocomposites

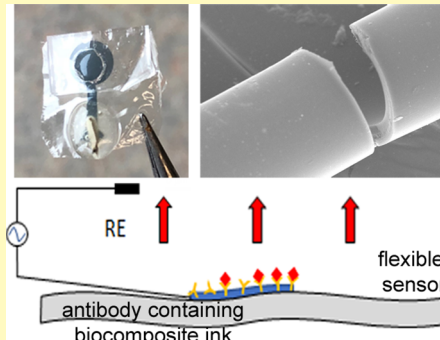
Meng Xu and Vamsi K. Yadavalli*^{†,ID}

Department of Chemical and Life Science Engineering, Virginia Commonwealth University, 601 W. Main Street, Richmond, Virginia 23284, United States

 Supporting Information

ABSTRACT: To expand the applications of flexible biosensors in point-of-care healthcare applications beyond monitoring of biophysical parameters, it is important to devise strategies for the detection of various proteins and biomarkers. Here, we demonstrate a flexible, fully organic, biodegradable, label-free impedimetric biosensor for the critical biomarker, vascular endothelial growth factor (VEGF). This biosensor was constructed by photolithographically patterning a conducting ink consisting of a photoreactive silk sericin coupled with a conducting polymer. These functional electrodes are printed on flexible fibroin substrates that are controllably thick and can be free-standing, or conform to soft surfaces. Detection was accomplished via the antibody to VEGF which was immobilized within the conducting matrix. The results indicated that the developed flexible biosensor was highly sensitive and selective to the target protein, even in challenging biofluids such as human serum. The biosensors themselves are biocompatible and degradable. Through this work, the developed flexible biosensor based on a simple and label-free strategy can find practical applications in the monitoring of wound healing or early disease diagnosis.

KEYWORDS: flexible biosensor, vascular endothelial growth factor (VEGF), electrochemical impedance spectroscopy, silk protein, biomarker detection



Flexible biosensors have been gaining increasing attention, particularly in the fields of wearable and implantable POC monitoring systems for human health.^{1–4} Such devices comprise mechanically compliant supporting substrates, with sensing regions that can maintain their duty of signal transduction even when the system is under motion or physical deformation. In comparison to their rigid counterparts, flexible sensors are typically designed to functional at nonplanar, soft, and even nonstationary biointerfaces. This feature enables operation directly at sites of interest, and without the interrupting the normal activities of the wearer. However, to date, most flexible sensors have focused primarily on the measurement of biophysical parameters such as temperature, pH, heart rate, blood/intraocular pressure, etc.^{5–7} Similarly, small molecule chemical analytes, such as ions, glucose, cortisol, dopamine, etc. have been studied.^{8,9} In contrast, larger biomarkers, such as proteins and biomacromolecules have been relatively less explored, because of challenges in immobilizing the biorecognition elements (e.g., antibody, aptamer, etc.) and signal transduction on a flexible substrate.¹⁰ The development of mechanically flexible and conformable biosensors for the accurate detection and sensitive quantification of specific biomarkers in clinical diagnosis can be critical toward the evaluation of regular biological and pathological activities, or responses to therapeutic interventions.^{11–13}

Here, we report on biosensors for the important biomarker: the vascular endothelial growth factor (VEGF), using flexible silk protein matrices with a biocompatible, antibody-containing conducting ink. VEGF is a key protein regulator in angiogenesis, vasculogenesis, and endothelial cell growth.^{13,14} VEGF₁₆₅, the predominant isoform of VEGF_A, is involved in numerous types of cancer development and metastasis.^{11,13,15} It plays a pivotal role in pathological angiogenesis associated with tumor growth, with overexpression resulting in additional blood vessels to provide independent blood flow.^{11,16} Elevated levels of VEGF in human blood serum is often considered an important indicator of several diseases including cancers.^{17–19} Therefore, VEGF is a useful biomarker to demonstrate detection in various settings. Significant efforts have been directed toward this goal, including immunoassays,^{20,21} fluorescence imaging,²² and biosensors.^{15,17,23–25} While the enzyme-linked immunosorbent assay (ELISA) has a tendency to be the gold standard for clinical quantification of many protein biomarkers with low limits of detection (LODs) and good specificity,^{26–28} it is not ideal for point-of-care (POC) applications. Drawbacks include lack of portability, complex protocols with long assay time, difficulty for multiplexed sensing, and low cost-effectiveness.^{29,30} Therefore, other

Received: January 31, 2019

Accepted: April 8, 2019

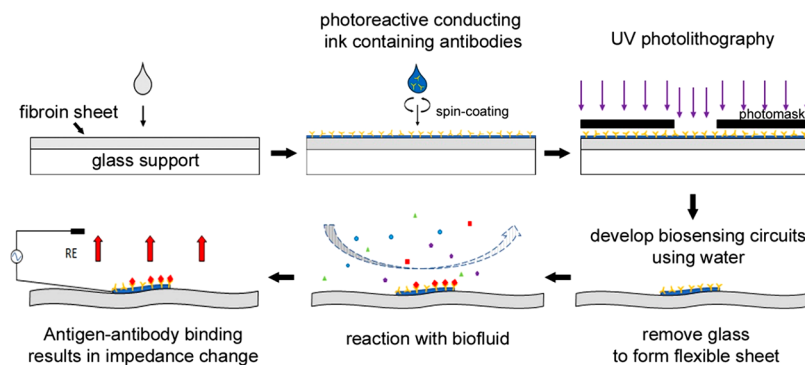
Published: April 8, 2019

Table 1. Some Representative Detection Strategies for VEGF^a

detection	strategy	recognition	target	LOD	linear range	ref
Impedimetric	Au electrode- MPA- VEGF receptor 1	VEGFR1	human VEGF	10 pg/mL	10–70 pg/mL	47
	Au-cysteamine-PAMAM-VEGFR1	VEGFR1	human VEGF	5 pg/mL	5–125 pg/mL	48
Differential Pulse Voltammetry	GCE/chitosan-rGO/thionine-Ab-VEGFR2-HRP	Anti-VEGFR2	VEGFR2	0.28 pM	0.4–86 pM	49
	Au electrode/GO-ssDNA-VEGF-Ab ₁ /PLLA/Ab ₂ -PSA	ssDNA	VEGF ₁₆₅	50 pg/mL	0.05–100 ng/mL	24
	Au electrode/MGO-Avastin	Avastin	human VEGF	31.25 pg/mL	31.25–2000 pg/mL	12
Amperometry	carbon fiber microelectrode-Fc-Ab-VEGF	anti-VEGF	VEGF	38 pg/mL	0–100 pg/mL	50
Field-effect transistor	SCG-based channel fabricated by LPCVD	multiplexed antibodies	ANXA3, ENO1, VEGF	0.1 pg/mL	1 pg/mL–1 µg/mL	51

^aAbbreviations used in this table: MPA, 3-mercaptopropionic acid; VEGFR1 and R2, VEGF receptor 1; VEGFR2, VEGF receptor 2; GCE, glassy carbon electrode; Ab, antibody; HRP, horseradish peroxidase; PSA, prostate specific antigen; PLLA, poly-L-lactic acid; Fc, ferrocene; MGO, magnetic graphene oxide; SCG, single crystalline graphene; and LPCVD, low-pressure chemical vapor deposition.

Scheme 1. Microfabrication of Flexible, Impedimetric Biosensor via Photolithography of Photo Fibroin and Sericin-Based Biocomposites



sensing strategies have attracted attention with high sensitivity, rapid response, small footprints, and multiplexed sensing capabilities, making them suitable for POC detection, and early disease diagnosis and monitoring. Table 1 shows a brief overview of some recently developed methodologies for VEGF detection.

To date, however, there remains a gap not only between laboratory-tested systems and clinical application, but also in new modalities of detection. In particular, no nonrigid (flexible or conformable) biosensors have been reported. Indeed, quantitative detection of protein biomarkers in flexible environments has not been widely shown. For the first time, we report on a flexible, impedimetric biosensor for the detection of VEGF₁₆₅ as a target protein biomarker. The biosensor is constructed on a photocross-linkable fibroin thin film that is mechanically flexible and conformable to soft tissue. The flexible biosensor was microfabricated using the previously reported silk protein photolithography technique.^{31,32} The sensing is accomplished using photolithographically micro-patterned electrodes of a conductive ink comprising photocrosslinkable sericin and the conducting polymer, poly(3,4-ethylenedioxythiophene): polystyrene sulfonate (PEDOT:PSS). VEGF sensing occurs via anti-VEGF₁₆₅ antibodies embedded in the ink forming a functional electrode. Unlike conventional, rigid protein sensors that require physical or chemical immobilization of antibodies on a surface,³³ the conductive ink ensures protection of the antibodies for the

capture of the targeted VEGF protein, as well as electrochemical performance. The use of electrochemical impedance spectroscopy (EIS) in the developed biosensor offers a rapid, simple, and label-free strategy to detect extremely low concentrations of VEGF. Sensing of the protein is demonstrated in various fluids (buffer, human serum, and simulated urine, with and without albumin), as well as under conditions of bending. The demonstrated flexible biosensor forms a promising modality for the broader detection of large protein targets in physiological environments or at biointerfaces.

MATERIALS AND METHODS

Materials. All reagents were at analytical grade unless stated otherwise. Silk fibroin was extracted and purified from *Bombyx mori* silkworm (Mulberry Farms, CA) based on previously reported protocols.³⁴ Silk sericin was purchased from Wako Chemicals (Osaka, Japan), and used as received. PEDOT:PSS (3%–4%) was purchased from Sigma-Aldrich (St. Louis, MO) and diluted to 1% when used. For the chemical modification of silk proteins, the reagents 2-isocyanatoethyl methacrylate (IEM, 98% with $\leq 0.1\%$ BHT as an inhibitor) and anhydrous lithium chloride (LiCl) were purchased from Sigma-Aldrich. Anhydrous dimethyl sulfoxide (DMSO), formic acid (FA), and simulated urine were purchased from Thermo Fisher Scientific (Waltham, MA). Polyclonal goat anti-VEGF antibody, VEGF₁₆₅ (recombinant, expressed in *E. coli*), and human serum (human male AB plasma, sterile-filtered) were purchased from Sigma-Aldrich.

Synthesis of Photoreactive Silk Proteins. Photoreactive fibroin (FPP) and sericin (SPP) were synthesized according the protocol

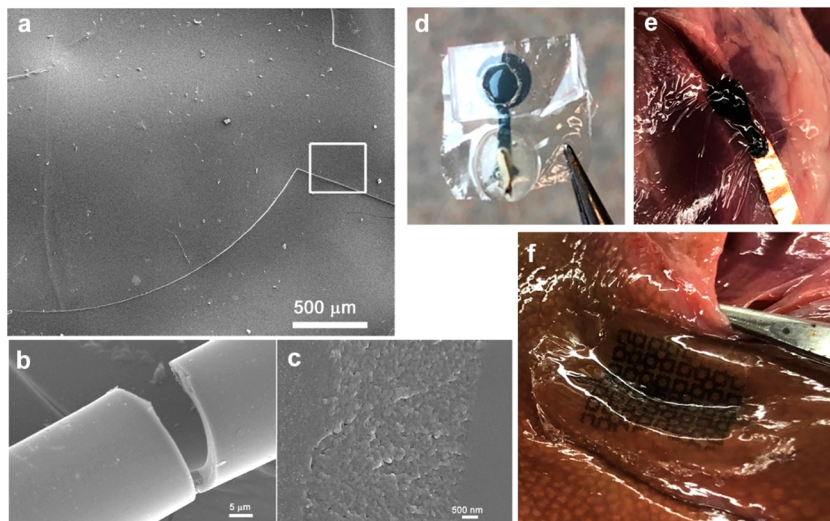


Figure 1. SEM images of (a) the sensor electrode, (b) the sensor electrode in a rolled-up condition, (c) closeup of the electrode surface marked by white rectangle in panel (a). The electrodes are 2–3 μm thick. (d) The free-standing biosensor is flexible and can be conformable to soft tissue (panels (e) and (f)) for potentially *in situ* detection of biomarkers at tissue interfaces. Various electrode configurations can be easily formed via photolithography.

previously reported by our group.^{31,35} Briefly, fibroin or sericin was dissolved in 1 M LiCl in DMSO to form 1% (w/v) solution. The proteins were conjugated with photoreactive methacrylate moieties through the reaction with IEM at 60 °C for 5 h with continuous N₂ purge. The modified proteins were precipitated in excess cold ethanol overnight. The precipitate was washed with cold ethanol/acetone (1:1) solution and centrifuged at 4 °C (three times). Finally, the product was lyophilized to obtain photoreactive and cross-linkable fibroin and sericin.

Fabrication of the Flexible Biosensor. Flexible fibroin substrates and conductive micropatterns were formed using contact photolithography (Scheme 1). FPP was dissolved completely in FA at 7.5% (w/v) concentration with 1.5% of Irgacure 2959 photoinitiator (BASF, Ludwigshafen, Germany). The FPP solution was then drop-cast on clean glass substrates. After the excess solvent was completely evaporated, the thin films were photopolymerized by UV exposure with an OmniCure S1000 UV Spot Curing lamp (Lumen Dynamics, Ontario, Canada) equipped with a 320–500 nm filter. The entire films were exposed at 365 nm (2 mW cm^{-2}) for 2.5 s. The biocomposite conductive ink containing 2.5% (w/v) of SPP, 1% (w/v) PEDOT:PSS, 1 $\mu\text{g mL}^{-1}$ of anti-VEGF₁₆₅ Ab, and 0.5% (v/v) of Darocur 1173 (Ciba Specialty Chemicals, Inc., Basel, Switzerland) was spin-coated on the FPP films (30 s, including an acceleration time of 10 s). After the spin-coating and solvent evaporation in darkness in a fume hood, the SPP/PEDOT:PSS/Ab conductive films results in a PEDOT:PSS concentration of ~28%. Patterned was performed under UV light for 1.5 s through a chrome photomask. The conductive pattern (electrode) was developed in DI water, followed by rinsing with excess water. The films themselves can be detached from the glass supports by immersing in water. Scanning electron microscopy (SEM) images were taken using a Hitachi SEM.

Electrochemical Impedance Measurement. EIS measurements were conducted using a Gamry Interface 1010E Potentiostat (Gamry Instruments, Warminster, PA). A standard three-electrode setup was used with Ag/AgCl and Pt electrodes as the reference and the counter electrodes, respectively. The fabricated flexible electrodes were used as the working electrode with silver paste and epoxy connects. The impedance spectra were recorded with an AC amplitude of 10 mV at a bias potential of 0 V, and the scanning frequency range of 1 Hz to 100 kHz. Incubation time to allow the capture of VEGF was 15 min. Equivalent circuit modeling was done using Gamry Echem Analyst software.

RESULTS AND DISCUSSION

Previously, we demonstrated photolithographically fabricated silk protein-conductive polymer-based flexible biosensors for the sensing of electrochemically active, small molecules such as ascorbic acid, glucose, and dopamine.^{31,32} These flexible biosensors are scalable, biocompatible, lightweight, easy-to-fabricate, and degradable. In order to extend the capabilities of such sensors as POC devices for healthcare, it is important to expand the repertoire of targets to large molecule biomarkers such as proteins which are typically *not electrochemically active*. This is difficult, because of not only the lack of an easily transduced signal, but also intrinsic challenges in capturing the analyte of interest (via recognition elements such as antibodies or aptamers). Specifically, these biorecognition agents need to be properly immobilized on surfaces, making it difficult if the substrate itself is flexible.^{33,36} This permits the development of wearable POC sensors that can *directly* detect protein biomarkers such as VEGF at biointerfaces or in biofluids.

Fabrication and Characterization of Flexible Bio-electrodes. Flexible fibroin substrates and conductive micropatterns were formed using contact photolithography (Scheme 1). UV light photolithography of a composite ink comprising the water soluble “photo-sericin” (sericin photoresist or SPP) and PEDOT:PSS (SPP/PEDOT:PSS) enables the formation of precise microscale features over macroscale areas. The silk sericin provides the biological matrix for the electrode, while also permitting easy fabrication. The “conducting polymer-carrier protein” micropatterns are then deposited and covalently attached to an underlying protein sheet comprised of a cross-linked photofibroin (FPP) to form a flexible and freestanding device. Because of the benign nature of the process (benchtop, room-temperature, aqueous), it is possible to disperse functional molecules such as antibodies within the conducting matrix resulting in a bioactive composite ink. Here, antibodies to the target VEGF were used to form the ink (SPP/PEDOT:PSS/Ab).

Figure 1 shows SEM images of the sensor electrodes. These mechanically flexible substrates can be rolled up and unrolled several times without any breakage. Most importantly, they can

be free-standing sensors that can perform detection untethered to any rigid surface. The sensors shown in Figure 1d are the ones used in the experiments discussed in this work. By making the substrate films controllably thick (10–100 μm), it is possible to form films that can adapt and conform, even to irregular surfaces. In prior work, we have shown that the entirely organic device, with no metal components, is biocompatible and controllably degradable (weeks to months) in the presence of proteolytic enzymes (the degradation of the electrodes is shown in Figure S1 in the Supporting Information).³⁷ This allows them to be conformable to soft tissue for the potential *in situ* detection of biomarkers at tissue interfaces (for instance, for measuring the extent of wound healing).³⁸ While in this work, we have not explicitly conducted sensing experiments at a tissue surface, the image (Figures 1e and 1f) shows representations on how this may occur with different electrode configurations, and will be the focus of subsequent research.

Electrochemical impedance spectroscopy (EIS) is used as a label free-surface characterization technique. The adaptation of EIS in this flexible biosensing system enables the ultrasensitive detection of VEGF using a single-step procedure. For the biosensor, the thickness of the SPP/PEDOT:PSS/Ab conductive electrodes is an important parameter, because it affects the electrochemical performance of the biosensor, as well as the exposure of the antibody for the capture of the target analyte (VEGF). Since the spin-coating rate determines the thickness of the conductive film, this was initially evaluated and optimized using EIS (Figure S2 in the Supporting Information). Based on the Nyquist plots at different spin-coating speeds, the electron transfer on the surface of the SPP/PEDOT:PSS/Ab conductive films is entirely mass-transfer-limited at low speeds (<500 rpm). While the thicker films were more conductive, they were not suitable for the detection of VEGF in this region. This is because the electron transfer resistance is mostly affected by the electrolyte transfer rate in the surrounding solution and not as much by the surface characteristics of the conductive films. The latter is what was altered in the event of the VEGF being captured by the antibody. At higher spin-coating speeds (1000 and 1500 rpm), thinner films are formed with higher impedance in PBS. The Nyquist plots show that a kinetically controlled regime appears, indicating that PEDOT:PSS, as the electron vehicle, is not enough to support the electron transfer for all electrolyte moved to the surface of the conductive films. Therefore, in this region, the electron transfer resistance would be significantly affected by the surface characteristics of the films, and thus proportional to the amount of VEGF bound to the antibody. A value of 1000 rpm for spin-coating was chosen in the following experiments, because it gave the optimized result between the electrochemical performance and the thickness of the conductive films. No leaching of the antibody was observed over several days, showing that the electrodes were stable. Imaging of the surface (Figure 1c) showed that the electrode surface was uniform at this speed.

Equivalent Circuit Modeling of the Biosensor. The impedance data were fitted into an equivalent circuit model (Figure 2a), which includes the bulk solution resistance (R_s), the electron-transfer resistance and double-layer capacitance at the reference electrode (R_{ref} and C_{ref}), the resistance and capacitance of the electrodes (R_{film} and C_{film}), and the electron-transfer resistance (R_{vegf}) and capacitance (C_{vegf}) that represent the interaction between the antibody and the target protein.

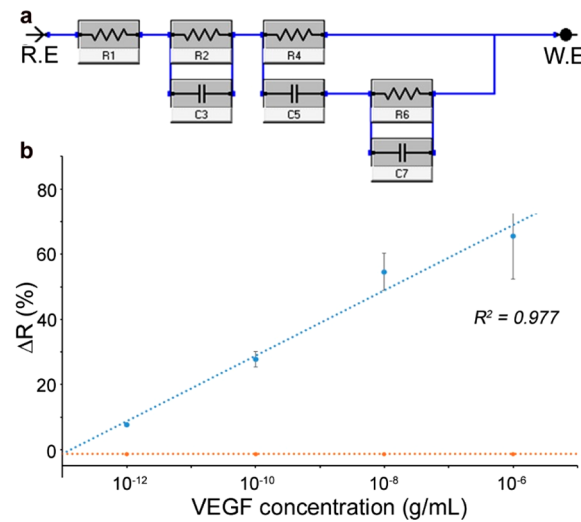


Figure 2. (a) The equivalent circuit model used to develop the corresponding sensor response to the added protein target. (R.E. = reference electrode, W.E. = working electrode). (b) The calibration curve for the detection VEGF in PBS buffer. The corresponding control shows sensor response with no addition of protein. All experiments were conducted in triplicate.

The configuration of the biosensor involves antibodies embedded in the conductive matrix of the electrodes. Therefore, the antibody molecules can be envisioned to work like “pin-holes” in the conductive matrix (SPP/PEDOT:PSS). Binding of the VEGF changes the resistance and capacitance of these “pin-holes”. As indicated in Table 2, the fitted results from the equivalent circuit model confirms that R_{vegf} showed significant changes due to the conjugation of VEGF (100 pg mL^{-1}), indicating that the capture of VEGF increases the charge transfer resistance of the system. In comparison, other elements showed no or very small changes. The goodness of fit (<0.00004 , with $p > 0.99$) suggests that this equivalent circuit model can well represent the electrochemical impedance system of the developed biosensor. Therefore, the R_{vegf} was analyzed to obtain calibration curves of sensor response versus the concentration of VEGF. The biosensors were tested in a variety of biologically relevant fluids.

Determination of VEGF in PBS Buffer Solution. The electrochemical responses of the sensors were initially studied in PBS (pH 7.4) (Figure 2b). Since the photolithographic patterning was performed in dry conditions, the electrodes were presaturated in buffer, following which they became stable for electrochemical measurements. The initial stability experiments showed that the impedance decreased in the first 15 min (as the SPP/PEDOT:PSS/Ab biocomposite equilibrated), following which they remained stable over several hours (Figure S3 in the Supporting Information). Therefore, electrodes were stored in buffer prior to reaction with VEGF. Ten microliters (10 μL) of different concentrations of VEGF were incubated, and the final detection was directly performed without any washing step after incubation. The same protocol for detection was followed in all experiments to mimic *in situ* readings. For comparison, the negative control (NC) used pure PBS for the incubation. As shown in Figure 2b, the normalized ΔR_{vegf} (which is defined as $\Delta R_{\text{vegf}} = (R_{\text{vegf}}^{t=15} - R_{\text{vegf}}^{t=0})/R_{\text{vegf}}^{t=0}$) of NC was $-3.34\% \pm 4.23\%$. The slight decrease of R_{vegf} in NC was likely caused by the continued diffusion of buffer into the conductive films. As previously

Table 2. Equivalent Circuit Model Fit of Sensor Response to VEGF (100 pg mL⁻¹).

	R_s (k Ω)	R_{ref} (k Ω)	C_{ref} (μ F)	R_{film} (k Ω)	C_{film} (nF)	R_{VEGF} (k Ω)	C_{VEGF} (pF)	goodness of fit
$T = 0$	3.59 ± 1.86	9.57 ± 4.33	34.4 ± 7.00	24.9 ± 1.90	17.1 ± 20.3	632 ± 30.8	4.31 ± 0.687	3.07×10^{-5}
$T = 15$ min	3.00 ± 1.87	9.78 ± 4.21	32.3 ± 6.98	25.7 ± 1.92	18.2 ± 24.7	693 ± 39.3	4.24 ± 0.657	3.93×10^{-5}

shown, there are small changes in the swelling and porosity of the conducting polymers due to electrochemical stimulation.³⁹ On the other hand, in the presence of protein, the biosensor showed a wide detection range from 1 pg mL⁻¹ to 1 μ g mL⁻¹ with a linear correlation between ΔR_{VEGF} and the VEGF concentration. The limit of detection (LOD) of VEGF in PBS was 1.03 pg mL⁻¹, with each experiment conducted in triplicate.

Determination of VEGF in Human Serum. To demonstrate the specific detection of VEGF using the developed biosensor, the device was tested in samples of human serum. Human serum is the portion of human blood free of red and white blood cells and platelets, as well as clotting proteins such as fibrinogen and prothrombin.⁴⁰ It is a complex aqueous solution (~95% water) containing a variety of biological and chemical substances such as proteins (albumins, globulins, lipoproteins, enzymes, and hormones), nutrients (carbohydrates, lipids, and amino acids), electrolytes, organic wastes, and other small organic molecules. It represents a useful solution to test the specificity of the developed biosensor against all the interferences mentioned above, as well as its resistance to biofouling. Samples of serum were spiked with different concentration of VEGF. The background noise from the original human serum was tested by using the original serum sample without any addition of VEGF. The results (Figure 3) showed that, even in serum, the

predictor for chronic kidney disease (CKD) progression in patients.^{44,45} The urinary excretion of VEGF has been reported showing significant elevation for patients with worsening or at advanced stage of CKD, in comparison to healthy controls. Besides a water content of ~91%–96%, urine from healthy individuals also contains urea, creatinine, inorganic salts (sodium, potassium), organic compounds (proteins, hormones, metabolites).⁴⁶ While a flexible sensor is not necessarily needed for urine testing, in this work, we studied the viability of using this sensor to detect VEGF. As above, it demonstrates the stability and specificity of the sensor in different challenging environments. Two types of artificial urine (AU) were tested: control (AUC) and urine containing albumin (AUA). These samples were spiked with VEGF. From the results (Figure 4), the sensor response to VEGF in both

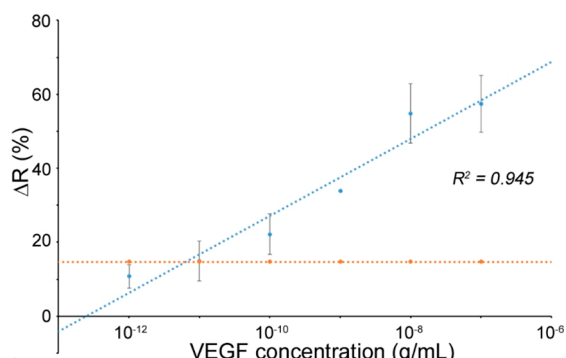


Figure 3. Calibration curve for the detection of VEGF in human serum. The corresponding control shows sensor response with no addition of protein. All experiments were conducted in triplicate.

sensor has a wide detection range, from 1 pg mL⁻¹ to 100 ng mL⁻¹, where the normalized ΔR_{VEGF} has a linear relationship to the concentration of VEGF in human serum. This detection range can very well cover the cutoff levels of serum VEGF in patients with certain types of cancer, which has been reported to range from 0.1 ng mL⁻¹ to 1 ng mL⁻¹.^{41–43} The control samples showed ΔR_{VEGF} of $11.84 \pm 4.44\%$, which is much higher than that of the sensor when used in PBS, indicating that the compounds in the human serum has larger interference on VEGF sensing. The LOD of the sensor to detect VEGF in human serum is 81.46 pg mL⁻¹.

Determination of VEGF in (Artificial) Urine. Recent studies have noted that VEGF could serve as an important

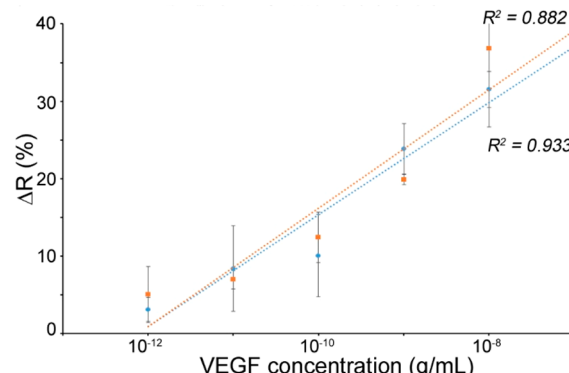


Figure 4. Sensor response in artificial urine (with and without albumin). The negative controls for both artificial urine samples are original samples without the addition of VEGF. The ΔR of artificial urine control was $5.87 \pm 1.71\%$, and the ΔR of artificial urine with albumin was $2.62 \pm 3.00\%$. All experiments were conducted in triplicate.

AU samples showed high compliance to each other, indicating that the interference of albumin in the artificial urine did not affect the sensor for the detection of VEGF. The ΔR values of AUC and AUA were $5.87 \pm 1.71\%$ and $2.62 \pm 3.00\%$, respectively. The sensor response to different concentrations of VEGF in these two types of artificial urine showed a very good linear regression in the range of 1 pg mL⁻¹ to 10 ng mL⁻¹. The limits of detection (LODs) of the sensor to detect VEGF in AUC and AUA were 22.22 pg mL⁻¹ and 24.87 pg mL⁻¹, respectively ($S/N = 3$). In comparison to previous reported works (Table 1), it is evident that this flexible biosensor presents very competitive metrics in various biologically relevant fluids, without the need for additional passivation.

Mechanical Stability under Flexure. While the sensors are observed to be free-standing and flexible, the stability of performance was tested under conditions of mechanical bending to demonstrate the effectiveness of the developed flexible biosensors. It is further important to stress that all the experiments discussed above were conducted with a freely suspended sensor film (without any rigid support as seen in Figure 1d). The unstressed (no bending) and stressed (30°,

45°, and 90° bends were studied) electrodes were measured for their overall impedance (Figure 5). Overall, only a very

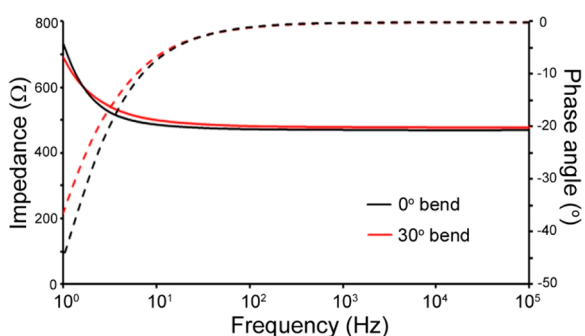


Figure 5. EIS spectra following mechanical bending of the biosensor. The solid and dotted lines represent the magnitude and the phase angle of impedance, respectively. The electrochemical impedance of the biosensor was measured in 1× PBS at different frequencies at no bending (0°) and inward bending (30°) states.

slightly increased magnitude of impedance (~200 Ω) was observed (results for 45° and 90° bends are presented in the Figure S4 in the Supporting Information). The phase angle of the impedance is relatively featureless and showed negligible changes before and after mechanical bending, indicating that the characteristics of the electrochemical system were not significantly altered. Considering the intended locations of use for such flexible biosensors, it is clear that such extreme bending would likely not be encountered. Nonetheless, these experiments show the overall stability of the system to mechanical challenge and robustness for operation under nonplanar conditions.

CONCLUSION

In summary, here we show a highly sensitive and flexible, label-free biosensor for the detection of the protein biomarker VEGF. The sensor was fabricated using photolithography to form functional microelectrodes on a flexible support film of silk fibroin. The electrodes themselves are fully organic, comprising a silk protein in conjunction with the conducting polymer PEDOT:PSS and the biorecognition element (antibody to VEGF). In contrast to rigid biosensors in which the antibodies are covalently bound to surfaces, limiting their application, here the antibodies were dispersed in the conducting matrix that not only confer protection but also enable the sensors to be used in freely suspended forms. This permits the sensors to be mechanically compliant and conformable to soft tissue for the impedimetric detection of protein biomarkers *in situ*. A range of biologically relevant fluids (buffer, serum, and urine) were demonstrated, showing the high sensitivity (pg/mL) and selectivity of the biosensor. Relatively small deviations of using the developed sensor in different media also indicate high reproducibility, which is important for the implementation as POC devices. Future experiments will focus on directly applying the systems to soft tissue or wound sites for the detection of VEGF and other relevant protein biomarkers, thereby expanding the range and utility of point-of-care devices used in personal healthcare applications.

ASSOCIATED CONTENT

Supporting Information

The Supporting Information is available free of charge on the ACS Publications website at DOI: [10.1021/acssensors.9b00230](https://doi.org/10.1021/acssensors.9b00230).

Flexible biosensors for the impedimetric detection of protein targets using silk-conductive polymer biocomposites; optical images showing gradual proteolytic degradation of SPP/PEDOT:PSS electrodes (Figure S1); optimization of the developed biosensor (Figures S2 and S3); additional electrochemical impedimetric characterization of the flexible electrodes under bending (Figure S4) ([PDF](#))

AUTHOR INFORMATION

Corresponding Author

*E-mail: vyadavalli@vcu.edu.

ORCID

Vamsi K. Yadavalli: [0000-0002-8879-1948](#)

Notes

The authors declare no competing financial interest.

ACKNOWLEDGMENTS

This research was partly supported by funding from the National Science Foundation (No. CBET-1704435). SEM images were obtained at the VCU Nanomaterials Characterization Center.

REFERENCES

- Wang, X. W.; Liu, Z.; Zhang, T. Flexible Sensing Electronics for Wearable/Attachable Health Monitoring. *Small* **2017**, *13* (25), 1602790.
- Wang, L.; Chen, D.; Jiang, K.; Shen, G. New insights and perspectives into biological materials for flexible electronics. *Chem. Soc. Rev.* **2017**, *46* (22), 6764–6815.
- Feiner, R.; Dvir, T. Tissue-electronics interfaces: from implantable devices to engineered tissues. *Nat. Rev. Mater.* **2017**, *3* (1), 17076.
- Xu, M.; Obodo, D.; Yadavalli, V. K. The design, fabrication, and applications of flexible biosensing devices. *Biosens. Bioelectron.* **2019**, *124–125*, 96–114.
- Heikenfeld, J.; Jajack, A.; Rogers, J.; Gutruf, P.; Tian, L.; Pan, T.; Li, R.; Khine, M.; Kim, J.; Wang, J.; Kim, J. Wearable sensors: modalities, challenges, and prospects. *Lab Chip* **2018**, *18* (2), 217–248.
- Bonato, P. Wearable Sensors and Systems. *IEEE Eng. Med. Biol. Mag.* **2010**, *29* (3), 25–36.
- Schwartz, G.; Tee, B. C. K.; Mei, J.; Appleton, A. L.; Kim, D. H.; Wang, H.; Bao, Z. Flexible polymer transistors with high pressure sensitivity for application in electronic skin and health monitoring. *Nat. Commun.* **2013**, *4*, 1859.
- Windmiller, J. R.; Wang, J. Wearable Electrochemical Sensors and Biosensors: A Review. *Electroanalysis* **2013**, *25* (1), 29–46.
- Mahesh, K. P. O.; Shown, I.; Chen, L.-C.; Chen, K.-H.; Tai, Y. Flexible sensor for dopamine detection fabricated by the direct growth of α -Fe₂O₃ nanoparticles on carbon cloth. *Appl. Surf. Sci.* **2018**, *427* (Part B), 387–395.
- Kamakoti, V.; Panneer Selvam, A.; Radha Shanmugam, N.; Muthukumar, S.; Prasad, S. Flexible Molybdenum Electrodes towards Designing Affinity Based Protein Biosensors. *Biosensors* **2016**, *6* (3), 36.
- Dehghani, S.; Nosrati, R.; Yousefi, M.; Nezami, A.; Soltani, F.; Taghdisi, S. M.; Abnous, K.; Alibolandi, M.; Ramezani, M. Aptamer-based biosensors and nanosensors for the detection of vascular

endothelial growth factor (VEGF): A review. *Biosens. Bioelectron.* **2018**, *110*, 23–37.

(12) Lin, C.-W.; Wei, K.-C.; Liao, S.-s.; Huang, C.-Y.; Sun, C.-L.; Wu, P.-J.; Lu, Y.-J.; Yang, H.-W.; Ma, C.-C. M. A reusable magnetic graphene oxide-modified biosensor for vascular endothelial growth factor detection in cancer diagnosis. *Biosens. Bioelectron.* **2015**, *67*, 431–437.

(13) Ferrara, N.; Gerber, H.-P.; LeCouter, J. The biology of VEGF and its receptors. *Nat. Med.* **2003**, *9*, 669.

(14) Olsson, A.-K.; Dimberg, A.; Kreuger, J.; Claesson-Welsh, L. VEGF receptor signalling in control of vascular function. *Nat. Rev. Mol. Cell Biol.* **2006**, *7*, 359.

(15) Li, J.; Sun, K.; Chen, Z.; Shi, J.; Zhou, D.; Xie, G. A fluorescence biosensor for VEGF detection based on DNA assembly structure switching and isothermal amplification. *Biosens. Bioelectron.* **2017**, *89*, 964–969.

(16) Ferrara, N. Vascular Endothelial Growth Factor: Basic Science and Clinical Progress. *Endocr. Rev.* **2004**, *25* (4), 581–611.

(17) Freeman, R.; Girsh, J.; Fang-ju Jou, A.; Ho, J. A.; Hug, T.; Dernedde, J.; Willner, I. Optical Aptasensors for the Analysis of the Vascular Endothelial Growth Factor (VEGF). *Anal. Chem.* **2012**, *84* (14), 6192–6198.

(18) Hsu, C.-L.; Lien, C.-W.; Wang, C.-W.; Harroun, S. G.; Huang, C.-C.; Chang, H.-T. Immobilization of aptamer-modified gold nanoparticles on BiOCl nanosheets: Tunable peroxidase-like activity by protein recognition. *Biosens. Bioelectron.* **2016**, *75*, 181–187.

(19) Sung, J.; Barone, P. W.; Kong, H.; Strano, M. S. Sequential delivery of dexamethasone and VEGF to control local tissue response for carbon nanotube fluorescence based micro-capillary implantable sensors. *Biomaterials* **2009**, *30* (4), 622–631.

(20) Ko, J.; Lee, S.; Lee, E. K.; Chang, S.-I.; Chen, L.; Yoon, S.-Y.; Choo, J. SERS-based immunoassay of tumor marker VEGF using DNA aptamers and silica-encapsulated hollow gold nanospheres. *Phys. Chem. Chem. Phys.* **2013**, *15* (15), 5379–5385.

(21) Sosic, A.; Meneghelli, A.; Antognoli, A.; Cretaiu, E.; Gatto, B. Development of a Multiplex Sandwich Aptamer Microarray for the Detection of VEGF165 and Thrombin. *Sensors* **2013**, *13* (10), 13425.

(22) Shan, S.; He, Z.; Mao, S.; Jie, M.; Yi, L.; Lin, J.-M. Quantitative determination of VEGF165 in cell culture medium by aptamer sandwich based chemiluminescence assay. *Talanta* **2017**, *171*, 197–203.

(23) Kwon, O. S.; Park, S. J.; Jang, J. A high-performance VEGF aptamer functionalized polypyrrole nanotube biosensor. *Biomaterials* **2010**, *31* (17), 4740–4747.

(24) Pan, L.-H.; Kuo, S.-H.; Lin, T.-Y.; Lin, C.-W.; Fang, P.-Y.; Yang, H.-W. An electrochemical biosensor to simultaneously detect VEGF and PSA for early prostate cancer diagnosis based on graphene oxide/ssDNA/PLLA nanoparticles. *Biosens. Bioelectron.* **2017**, *89*, 598–605.

(25) Kwon, O. S.; Park, S. J.; Hong, J.-Y.; Han, A. R.; Lee, J. S.; Lee, J. S.; Oh, J. H.; Jang, J. Flexible FET-Type VEGF Aptasensor Based on Nitrogen-Doped Graphene Converted from Conducting Polymer. *ACS Nano* **2012**, *6* (2), 1486–1493.

(26) Kingsmore, S. F. Multiplexed protein measurement: technologies and applications of protein and antibody arrays. *Nat. Rev. Drug Discovery* **2006**, *5* (4), 310–320.

(27) Lilja, H.; Ulmert, D.; Vickers, A. J. Prostate-specific antigen and prostate cancer: prediction, detection and monitoring. *Nat. Rev. Cancer* **2008**, *8*, 268.

(28) Williams, T. I.; Toups, K. L.; Saggese, D. A.; Kalli, K. R.; Cliby, W. A.; Muddiman, D. C. Epithelial Ovarian Cancer: Disease Etiology, Treatment, Detection, and Investigational Gene, Metabolite, and Protein Biomarkers. *J. Proteome Res.* **2007**, *6* (8), 2936–2962.

(29) Topkaya, S. N.; Azimzadeh, M.; Ozsoz, M. Electrochemical Biosensors for Cancer Biomarkers Detection: Recent Advances and Challenges. *Electroanalysis* **2016**, *28* (7), 1402–1419.

(30) Munge, B. S.; Stracensky, T.; Gamez, K.; DiBiase, D.; Rusling, J. F. Multiplex Immunosensor Arrays for Electrochemical Detection of Cancer Biomarker Proteins. *Electroanalysis* **2016**, *28* (11), 2644–2658.

(31) Pal, R. K.; Farghaly, A. A.; Collinson, M. M.; Kundu, S. C.; Yadavalli, V. K. Photolithographic Micropatterning of Conducting Polymers on Flexible Silk Matrices. *Adv. Mater.* **2016**, *28* (7), 1406–1412.

(32) Pal, R. K.; Farghaly, A. A.; Wang, C.; Collinson, M. M.; Kundu, S. C.; Yadavalli, V. K. Conducting polymer-silk biocomposites for flexible and biodegradable electrochemical sensors. *Biosens. Bioelectron.* **2016**, *81*, 294–302.

(33) Sharma, S.; Byrne, H.; O'Kennedy, R. J. Antibodies and antibody-derived analytical biosensors. *Essays Biochem.* **2016**, *60* (1), 9–18.

(34) Rockwood, D. N.; Preda, R. C.; Yücel, T.; Wang, X.; Lovett, M. L.; Kaplan, D. L. Materials fabrication from *Bombyx mori* silk fibroin. *Nat. Protoc.* **2011**, *6*, 1612.

(35) Kurland, N. E.; Dey, T.; Kundu, S. C.; Yadavalli, V. K. Precise Patterning of Silk Microstructures Using Photolithography. *Adv. Mater.* **2013**, *25* (43), 6207–6212.

(36) Trilling, A. K.; Beekwilder, J.; Zuilhof, H. Antibody orientation on biosensor surfaces: a minireview. *Analyst* **2013**, *138* (6), 1619–1627.

(37) Pal, R. K.; Kundu, S. C.; Yadavalli, V. K. Fabrication of flexible, fully organic, degradable energy storage devices using silk proteins. *ACS Appl. Mater. Interfaces* **2018**, *10* (11), 9620–9628.

(38) Bao, P.; Kodra, A.; Tomic-Canic, M.; Golinko, M. S.; Ehrlich, H. P.; Brem, H. The role of vascular endothelial growth factor in wound healing. *J. Surg. Res.* **2009**, *153* (2), 347–358.

(39) Smela, E. Conjugated polymer actuators for biomedical applications. *Adv. Mater.* **2003**, *15* (6), 481–494.

(40) Psychogios, N.; Hau, D. D.; Peng, J.; Guo, A. C.; Mandal, R.; Bouatra, S.; Sinelnikov, I.; Krishnamurthy, R.; Eisner, R.; Gautam, B.; Young, N.; Xia, J.; Knox, C.; Dong, E.; Huang, P.; Hollander, Z.; Pedersen, T. L.; Smith, S. R.; Bamforth, F.; Greiner, R.; McManus, B.; Newman, J. W.; Goodfriend, T.; Wishart, D. S. The Human Serum Metabolome. *PLoS One* **2011**, *6* (2), e16957.

(41) Chin, K. F.; Greenman, J.; Gardiner, E.; Kumar, H.; Topping, K.; Monson, J. Pre-operative serum vascular endothelial growth factor can select patients for adjuvant treatment after curative resection in colorectal cancer. *Br. J. Cancer* **2000**, *83*, 1425.

(42) Hyodo, I.; Doi, T.; Endo, H.; Hosokawa, Y.; Nishikawa, Y.; Tanimizu, M.; Jinno, K.; Kotani, Y. Clinical significance of plasma vascular endothelial growth factor in gastrointestinal cancer. *Eur. J. Cancer* **1998**, *34* (13), 2041–2045.

(43) Li, L.; Wang, L.; Zhang, W.; Tang, B.; Zhang, J.; Song, H.; Yao, D.; Tang, Y.; Chen, X.; Yang, Z.; Wang, G.; Li, X.; Zhao, J.; Ding, H.; Reed, E.; Li, Q. Q. Correlation of Serum VEGF Levels with Clinical Stage, Therapy Efficacy, Tumor Metastasis and Patient Survival in Ovarian Cancer. *Anticancer Res.* **2004**, *24* (3B), 1973–1979.

(44) Agarwal, R.; Duffin, K. L.; Laska, D. A.; Voelker, J. R.; Breyer, M. D.; Mitchell, P. G. A prospective study of multiple protein biomarkers to predict progression in diabetic chronic kidney disease. *Nephrol., Dial., Transplant.* **2014**, *29* (12), 2293–2302.

(45) Kim, S. H.; Jung, Y. J.; Kang, K. P.; Lee, S.; Park, S. K.; Lee, J.-H.; Kim, N. H.; Kim, W. Decreased serum level and increased urinary excretion of vascular endothelial growth factor-C in patients with chronic kidney disease. *Kidney Res. Clin. Pract.* **2013**, *32* (2), 66–71.

(46) Rose, C.; Parker, A.; Jefferson, B.; Cartmell, E. The Characterization of Feces and Urine: A Review of the Literature to Inform Advanced Treatment Technology. *Crit. Rev. Environ. Sci. Technol.* **2015**, *45* (17), 1827–1879.

(47) Sezgintürk, M. K. A new impedimetric biosensor utilizing VEGF receptor-1 (Flt-1): Early diagnosis of vascular endothelial growth factor in breast cancer. *Biosens. Bioelectron.* **2011**, *26* (10), 4032–4039.

(48) Sezgintürk, M. K.; Uygun, Z. O. An impedimetric vascular endothelial growth factor biosensor-based PAMAM/cysteamine-modified gold electrode for monitoring of tumor growth. *Anal. Biochem.* **2012**, *423* (2), 277–285.

(49) Wei, T.; Tu, W.; Zhao, B.; Lan, Y.; Bao, J.; Dai, Z. Electrochemical monitoring of an important biomarker and target protein: VEGFR2 in cell lysates. *Sci. Rep.* **2015**, *4*, 3982.

(50) Prabhulkar, S.; Alwarappan, S.; Liu, G.; Li, C.-Z. Amperometric micro-immunosensor for the detection of tumor biomarker. *Biosens. Bioelectron.* **2009**, *24* (12), 3524–3530.

(51) Li, P.; Zhang, B.; Cui, T. Towards intrinsic graphene biosensor: A label-free, suspended single crystalline graphene sensor for multiplex lung cancer tumor markers detection. *Biosens. Bioelectron.* **2015**, *72*, 168–174.